

Determining the mass loss limit for close-in exoplanets: What can we learn from transit observations?

H. Lammer¹, P. Odert², M. Leitzinger², M. L. Khodachenko¹, M. Panchenko¹,
Yu. N. Kulikov³, T. L. Zhang¹, H. I. M. Lichtenegger¹, N. V. Erkaev⁴, G. Wuchterl⁵, G. Micela⁶,
T. Penz⁷, J. Weingrill¹, M. Steller¹, H. Ottacher¹, J. Hasiba¹, and A. Hanslmeier²

¹ Space Research Institute, Austrian Academy of Sciences, Schmiedlstrasse 6, A-8042 Graz, Austria

² Institute for Physics, IGAM, University of Graz, Universitätsplatz 3, A-8010 Graz, Austria

³ Polar Geophysical Institute, Russian Academy of Sciences, Khalturina 15, 183010 Murmansk, Russian Federation

⁴ Institute for Computational Modelling, Russian Academy of Sciences, and Siberian Federal University, Krasnoyarsk, Russian Federation

⁵ Thüringer Landessternwarte Tautenburg, Sternwarte 5 D-07778 Tautenburg, Germany

⁶ INAF - Osservatorio Astronomico, Piazza del Parlamento 1, I-90134 Palermo, Italy

⁷ On leave from the INAF - Osservatorio Astronomico, Palermo, Italy

Received February 23, 2009

ABSTRACT

Aims. We study the possible atmospheric mass loss of 49 known transiting exoplanets around F, G, K, and M-type stars over evolutionary time scales. Furthermore, for stellar wind induced mass loss studies we estimate the position of the pressure balance boundary between Coronal Mass Ejection (CME) and stellar wind ram pressures and the planetary ionosphere pressure for non- or weakly magnetized gas giants at close orbits.

Methods. The thermal mass loss of atomic hydrogen is calculated by modifying the energy-limited equation with a realistic heating efficiency, a radius-scaling law and a mass loss enhancement factor of the Roche lobe. The model takes into account the temporal evolution of the stellar XUV flux, by applying power laws for F, G, K, and M-type stars. The planetary ionopause obstacle, which is a relevant factor for ion pick up escape of non- or weakly magnetized gas giants is estimated, by applying empirical power-laws.

Results. We found that WASP-12 b may have lost about 20–25 %. Several transiting low density gas giants at similar orbital location, like CoRoT-Exo-1 b lost about 5–7 % of their initial mass. All other transiting exoplanets in our sample experience negligible thermal mass loss ($\leq 2\%$) during their life time. We found that the ionospheric pressure can balance the colliding dense stellar wind and average CME plasma flows at distances which are above the visual radius of “Hot Jupiters”, resulting in mass losses $< 2\%$ during evolutionary time scales. The ram pressure of fast CMEs can not be balanced by the ionospheric plasma pressure at orbital distances between 0.02–0.1 AU. Therefore, collisions between hot gas giants and fast CMEs result in large atmospheric mass loss, which may influence the mass evolution of gas giants with masses $< M_{\text{Jup}}$. Depending on stellar spectral type, planetary density, heating efficiency, orbital distance, and the related Roche lobe effect we expect that at distances between 0.015–0.02 AU Jupiter-class and sub-Jupiter-class exoplanets can loose several tens of percent of their initial mass. At orbital distances ≤ 0.015 AU hot gas giants in orbits around solar type stars may even evaporate down to their core-size, while low density Neptune-class objects can loose their hydrogen envelopes at orbital distances ≤ 0.045 AU.

Key words. exoplanets – thermal and non-thermal mass loss – evaporation boundary – ionopause location

1. Introduction

The upper atmospheres of short periodic exoplanets are affected strongly by the X-ray and EUV (XUV) radiation as well as the dense plasma environment of their host stars. Therefore, these exoplanets experience high thermal (Lammer et al. 2003; Vidal-Madjar et al. 2003; Lecavelier-des Etangs et al. 2004; Yelle 2004, 2006; Baraffe et al. 2004; Tian et al. 2005; Erkaev et al. 2007; Lecavelier Des Etangs 2007; Muñoz 2007; Penz et al. 2008a, 2008b; Penz and Micela 2008) and non-thermal (Erkaev et al. 2005; Khodachenko et al. 2007) atmospheric mass loss over their lifetime.

Khodachenko et al. (2007) studied the expected minimum and maximum possible atmospheric H^+ pick up erosion of the “Hot Jupiter” HD209458 b due to stellar Coronal Mass Ejections (CMEs) and concluded that hydrogen-rich gas giants, which orbit around solar-like stars at distances ≤ 0.05 AU should have been strongly eroded if the upper atmospheres are not

protected by a magnetosphere. This magnetosphere should be strong enough, so that the stellar plasma flow can be deflected at distances $> 1.5 r_{\text{pl}}$ above the radius. These authors found that stellar wind induced H^+ pick up loss can erode a “Hot Jupiter” to its core-size if the ionopause obstacle would form at distances of $\leq 1.3 r_{\text{pl}}$ above the planet of the effected planet. This non-thermal mass loss process depends on the strengths of the intrinsic magnetic moments. Grießmeier et al. (2004) estimated for slow rotating tidally locked “Hot Jupiters” that their magnetic moments should be in a range between $0.005 - 0.1 M_{\text{Jup}}$. From this study one can expect that weakly magnetized short periodic gas giants, which experience a Venus-like stellar plasma–atmosphere interaction should exist.

However, Yamauchi and Wahlund (2007) investigated the response of the ionopause location as function of solar XUV radiation and concluded that the ionopause obstacle may always form at altitudes which are close or above the exobase level.

Comparative spacecraft observations of Earth, Venus and Mars indicate a large variation of ionospheric density and ionopause location between solar minimum and maximum conditions (e.g. Evans 1977; Zhang et al. 1990; Kliore and Luhmann 1991). All planetary bodies in the Solar System with substantial atmospheres (e.g. Earth, Venus, Mars, and Titan) produce ionospheres which expand above the exobase. Therefore, one can also expect that the extreme XUV exposed and hydrodynamically expanding thermospheres of “Hot Jupiters” will also have a strong ionizing component, which may expand the ionopause up to distances where the ion pick up process could be less effective as suggested by Khodachenko et al. (2007).

The aim of this paper is to estimate the initial mass of 49 known transiting exoplanets¹ where the stellar and planetary parameters are well determined. Furthermore, we investigate at which orbital distances hydrogen-rich gas giants or “Hot Neptunes” can maintain their initial atmospheric hydrogen inventories, and at which distance they may experience huge atmospheric mass loss rates that can influence the expected short period exoplanet population (Wuchterl et al. 2007). Additionally to the thermal mass loss study we investigate if the ionospheric pressure of non- or weakly magnetized “Hot Jupiters” is strong enough to balance the ram pressure of the dense stellar wind and CME plasma flow at distances which are larger than the critical altitude of $\sim 1.5r_{\text{up}}$. Finally, we compare the efficiency of thermal and non-thermal mass loss processes with exoplanet observations and previous mass loss estimations.

2. Thermal atmospheric mass loss

The maximum possible thermal atmospheric mass loss rate L_{th} can be calculated by assuming that an atmosphere contains no efficient IR-cooling molecules (e.g., CO_2 , H_3^+ , etc.) in the thermosphere and by using the energy-limited equation (Lecavelier des Etangs 2007) which was originally derived for Earth-like planets by Sekiya et al. (1980a; 1980b; 1981) and Watson et al. (1981). Erkaev et al. (2007) and Lecavelier Des Etangs (2007) modified the energy-limited equation

$$L_{\text{th}} = \frac{\pi r_{\text{XUV}}^2 F_{\text{XUV}} \zeta(K)}{\Phi_0}, \quad (1)$$

for the application to close-in hydrogen-rich hot Jupiters which also includes a loss rate enhancement due to the closeness of the planet to the Roche lobe boundary, with

$$\zeta = \frac{1}{K(\xi)}, \quad (2)$$

where

$$\xi = \frac{r_{\text{Rl}}}{r_{\text{pl}}} = d \left(\frac{4\pi\rho_{\text{pl}}}{9M_*} \right)^{\frac{1}{3}}, \quad (3)$$

where Rl is the Roche lobe distance, r_{pl} the planetary radius, ρ_{pl} the planetary density, orbital distance d and stellar mass M_* . K is the non-linear potential energy reduction factor due to the stellar tidal forces (Erkaev et al. 2007)

$$K(\xi) = 1 - \frac{3}{2\xi} + \frac{1}{2\xi^3} < 1. \quad (4)$$

F_{XUV} is the stellar XUV flux at the planets orbit and $\Phi_0/\zeta(K)$ is the gravitational potential difference between r_{pl} and the first

Lagrange point r_{Rl} for a planet affected by stellar tidal forces. r_{XUV} is the distance in the thermosphere where the optical thickness $\tau_{\text{XUV}} \rightarrow 1$ and the main part of the XUV radiation is absorbed. One should note that r_{XUV} is close to the visual planetary radius and can therefore be substituted by r_{pl} (Yelle 2004).

Recently, Penz et al. (2008a) studied for the first time the thermal atmospheric mass loss of the low density gas giant HD209458 b over evolutionary time periods by applying a full hydrodynamic approach and found that the thermal mass loss rate can be approximated by the energy-limited approach if one introduces a heating efficiency factor. The heating efficiency factor reduces the mass loss which indicates that Lecavelier Des Etangs (2007) applying the energy-limited approach overestimated the escape rates in his study. To be conform with the full hydrodynamic approach, we include a heating efficiency η in Eq. (1) for the thermal atmospheric mass loss evolution studies. The thermal mass loss rate in units of g s^{-1} can be written as

$$\frac{dM_{\text{th}}}{dt} = \frac{\pi r_{\text{pl}}(t)^3 F_{\text{XUV}}(t) \eta \zeta(M_{\text{pl},t})}{GM_{\text{pl}}(t)}, \quad (5)$$

with the planetary mass M_{pl} and G the Newton gravitational constant. The minimum and maximum values of the heating efficiencies η related to XUV heated hydrogen-rich thermospheres found in the literature are in the range of 10 – 60 % (Chassefire, 1996; Yelle 2004; Tian et al. 2005). To study the influence of the heating efficiency on the thermal mass loss rates we use these values for η and compare the mass loss with $\eta=100\%$ for the energy limited approach.

Erkaev et al. (2007) showed that Eqs. (1) and (4) can be applied for close-in gas giants at orbital distances ≤ 0.15 AU, because due to the Roche lobe effect the upper atmospheres of such planets can also experience hydrodynamic blow-off conditions even if their exobase temperatures are lower than those required for blow-off in the case of the classic Newtonian gravitational potential. For very massive or Jupiter-class exoplanets exposed to less intense stellar XUV fluxes at orbital distances > 0.15 AU the exobase temperatures can be lower than the critical temperature for the onset of the blow-off. This will result in stable upper atmospheres which experience only Jeans escape.

Because the age of the majority of the host stars in our exoplanet sample is not well known, we assume that all stars have an average age of about 4 Gyr. We calculated the mass loss rates backwards to an initial age of 0.1 Gyr by using Eq. (4) with M_{pl} and r_{pl} being the mass and radius obtained from the transiting exoplanets.

Most previous works scaled the present-day solar XUV luminosity to closer orbital distances or, in evolutionary models, applied the scaling law for the temporal evolution of the stellar radiation derived by Ribas et al. (2005) from the “Sun in Time” program. The “Sun in Time” program is based on a small sample of solar proxies which allow the determination of this average scaling law for the XUV luminosity for a range of wavelength from 1–1200 Å. Penz et al. (2008b) pointed out that stars of the same spectral type show a broad distribution of the X-ray luminosity, which varies over a few orders of magnitude. Because of interstellar absorption and the lack of sensitive instruments this distribution can be observed only for the XUV wavelength in the range of 1–200 Å (e.g., Preibisch and Feigelson 2005).

In this study we use therefore, also the scaling laws given by Penz et al. (2008b) and Penz and Micela (2008) for the very extreme UV and X-ray luminosity evolution. These were constructed from the X-ray distributions of stars in the Pleiades and Hyades clusters. The temporal evolution of the stellar X-ray flux

¹ Extrasolar Planets Encyclopedia status February 2009; <http://www.exoplanet.eu/>

F_X at the planets' orbit and r_{pl} are taken into account, whereas the stellar mass M_* and orbital distance d is assumed to be constant. To account for the F and K stars in our sample we used the upper limit of G stars for the F star scaling law and the lower limit for K stars (cf. Penz et al. (2008b), Fig. 2). For F stars we use

$$L_X = \begin{cases} 0.284L_0t^{-0.547} & t \leq 0.6 \text{ Gyr} \\ 0.155L_0t^{-1.72} & t > 0.6 \text{ Gyr} \end{cases}, L_0 = 10^{29.83}, \quad (6)$$

for G stars

$$L_X = \begin{cases} 0.375L_0t^{-0.425} & t \leq 0.6 \text{ Gyr} \\ 0.19L_0t^{-1.69} & t > 0.6 \text{ Gyr} \end{cases}, L_0 = 10^{29.35}, \quad (7)$$

for K stars

$$L_X = \begin{cases} 0.474L_0t^{-0.324} & t \leq 0.6 \text{ Gyr} \\ 0.234L_0t^{-1.72} & t > 0.6 \text{ Gyr} \end{cases}, L_0 = 10^{28.87}, \quad (8)$$

and for M stars

$$L_X = \begin{cases} 0.17L_0t^{-0.77} & t \leq 0.6 \text{ Gyr} \\ 0.13L_0t^{-1.34} & t > 0.6 \text{ Gyr} \end{cases}, L_0 = 10^{28.75}, \quad (9)$$

with t in Gyr and L_X in erg s^{-1} where $F_X = L_X/4\pi d^2$. Because we study the expected mass losses over evolutionary time periods, we have to consider a mass-radius relation. We apply a scaling law which was developed by Lecavelier Des Etangs (2007) and fits the mass-radius relation given in Burrows et al. (2000) and Guillot (2005) for exoplanets with $M_{\text{pl}} \gtrsim 0.1M_{\text{Jup}}$

$$r_{\text{pl}}(t) = r_{\infty}(1 + \beta t^{-0.3}), \quad (10)$$

with t in Gyr, $\beta = 0.2$ for $M_{\text{pl}} \geq 0.3M_{\text{Jup}}$ and $\beta = 0.3$ for $M_{\text{pl}} \approx 0.1M_{\text{Jup}}$. For planets with $M_{\text{pl}} < 0.1M_{\text{Jup}}$ we also used $\beta = 0.3$.

Figs. 1–3 show the lost mass in % of initial planetary mass integrated over 4 Gyr for transiting exoplanets orbiting F, G and K-type host stars with a heating efficiency η of 60 %.

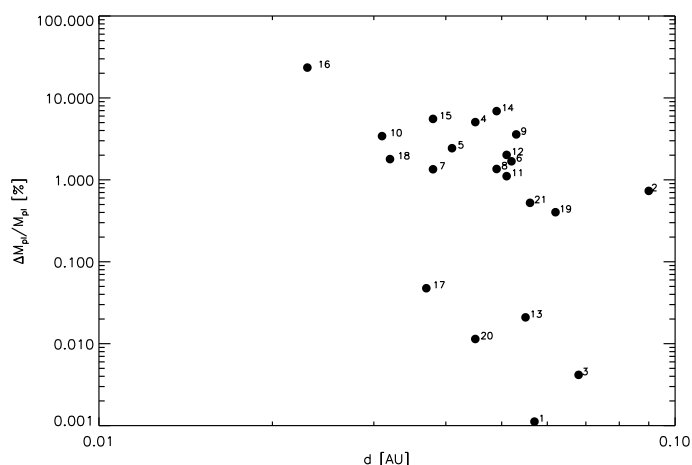


Fig. 1. Lost mass of transiting F-star exoplanets during 4 Gyr. The characteristics of the numbered exoplanets and their host stars can be found in Table 1.

Table 1 summarizes the planetary parameters of the 49 transiting exoplanets and the lost mass due to thermal evaporation over 4 Gyr corresponding to heating efficiencies of 10 %, 60 % and full energy-limited conditions with $\eta = 100$ %. As one can see from Fig. 1 and Table 1, from 21 F-star transiting exoplanets

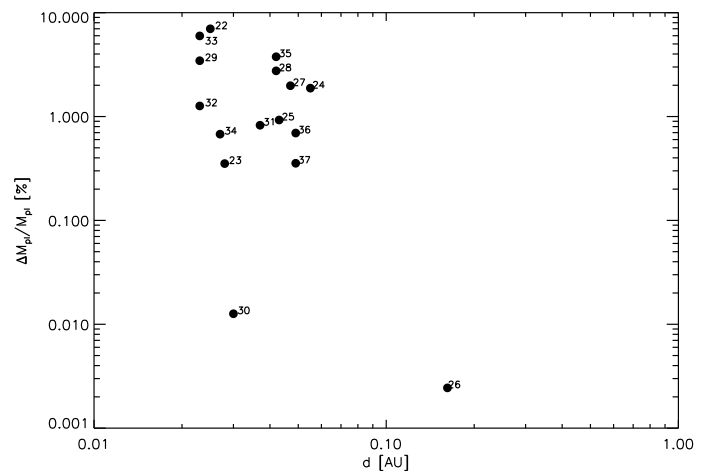


Fig. 2. Lost mass of transiting G-star exoplanets during 4 Gyr. The characteristics of the numbered exoplanets and their host stars can be found in Table 1.

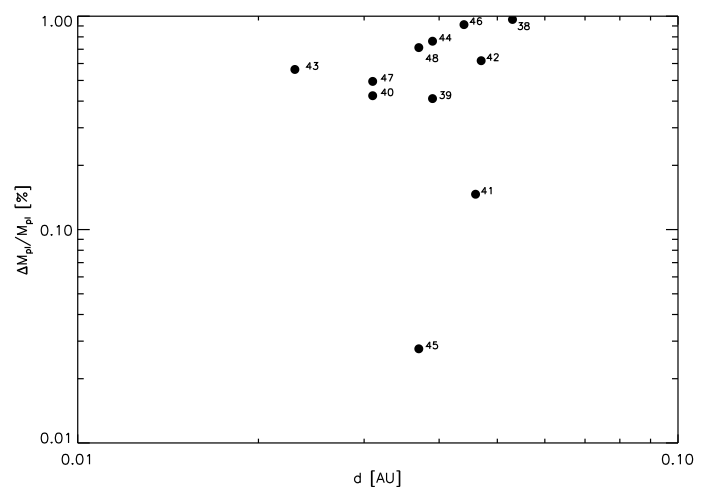


Fig. 3. Lost mass of transiting K-star exoplanets during 4 Gyr. The characteristics of the numbered exoplanets and their host stars can be found in Table 1.

only 6 lost ~ 4 –24 % of their initial masses. From our calculations WASP-12 b, which is also the closest of the F-star transit planet sample experienced the highest mass loss. The same exoplanet has also a low density of about 0.3 g cm^{-3} and the highest Roche lobe related mass loss enhancement factor ζ . TRES-4 b has the lowest density of about 0.2 g cm^{-3} at an orbit location of about 0.051 AU and shows the second largest mass loss of about 7 % of our F-star transit exoplanet sample.

Fig. 2 shows the lost mass of 16 transiting exoplanets in orbits around G-type stars. One can see that 7 exoplanets lost ~ 2 –7 % of their initial mass during 4 Gyr. From these 7 planets CoRoT-Exo-1 b lost about 7 % of its initial mass and is followed by WASP-4 b which lost about 6 % and OGLE-TR-56 b with about 3.5 %. All three exoplanets are low density planets and orbit at close distances between 0.0225–0.0254 AU. The other gas giants in our G star exoplanet sample have more or less negligible thermal mass loss rates.

Fig. 3 shows the lost mass of 12 exoplanets in orbits around K-type stars. Compared to the F and G star exoplanets the thermal mass loss of our planet samples in similar orbital distances around lower mass K and M-type stars (see Table 1) is negligible. This result is in agreement with Penz and Micela (2008),

Table 1. Masses and radii of 49 transiting exoplanets, stellar masses, as well as most of the spectral types are taken from the Extrasolar Planets Encyclopaedia; status February 2009; <http://www.exoplanet.eu/>. Spectral types which are roughly estimated corresponding to the mass sequence are indicated with a superscript x . The lost mass is calculated over a period of 4 Gyr for three different values of heating efficiency (10 %, 60 %, 100 %). The planetary densities and the Roche lobe related mass loss enhancement factor ζ are also given.

	Exoplanet	$M_{\text{pl}}/M_{\text{Jup}}$	$r_{\text{pl}}/r_{\text{Jup}}$	ρ_{pl}	$M_{\text{star}}/M_{\text{Sun}}$	spectral type	Distance	ζ	$\Delta M_{\text{pl}}/M_{\text{pl}}^{10\%}$	$\Delta M_{\text{pl}}/M_{\text{pl}}^{60\%}$	$\Delta M_{\text{pl}}/M_{\text{pl}}^{100\%}$
F		[g cm ⁻³]					[AU]		mass loss [%]		
1	CoRoT-Exo-3 b	21.66	1.01	26.08	1.37	F3V	0.06	1.08	0.0002	0.001	0.0017
2	CoRoT-Exo-4 b	0.72	1.19	0.53	1.1	F0V	0.09	1.19	0.12	0.73	1.212
3	HAT-P-2 b	8.62	0.95	12.43	1.29	F8	0.07	1.09	0.0007	0.004	0.0069
4	HAT-P-4 b	0.68	1.27	0.41	1.26	F	0.05	1.55	0.90	5.07	8.02
5	HAT-P-5 b	1.06	1.26	0.66	1.16	F ^x	0.04	1.48	0.42	2.43	3.95
6	HAT-P-6 b	1.06	1.33	0.56	1.29	F	0.05	1.39	0.28	1.68	2.75
7	HAT-P-7 b	1.77	1.36	0.87	1.47	F ^x	0.04	1.53	0.23	1.34	2.21
8	HAT-P-8 b	1.52	1.5	0.56	1.28	F ^x	0.05	1.42	0.23	1.35	2.23
9	HAT-P-9 b	0.78	1.4	0.35	1.28	F	0.05	1.48	0.63	3.58	5.76
10	OGLE-TR-132 b	1.14	1.18	0.86	1.26	F	0.03	1.67	0.6	3.42	5.5
11	OGLE-TR-182 b	1.01	1.13	0.87	1.14	F ^x	0.05	1.32	0.19	1.11	1.83
12	OGLE-TR-211 b	1.03	1.36	0.51	1.33	F ^x	0.05	1.43	0.35	2.02	3.29
13	SWEEPS-04	3.8	0.81	8.87	1.24	F ^x	0.06	1.12	0.003	0.02	0.04
14	TrES-4 b	0.92	1.79	0.2	1.38	F	0.05	1.70	1.27	6.9	10.73
15	WASP-1 b	0.89	1.36	0.44	1.24	F7V	0.04	1.69	1.0	5.54	8.73
16	WASP-12 b	1.41	1.79	0.31	1.35	F	0.02	3.68	5.97	23.46	31.23
17	WASP-14 b	7.73	1.26	4.8	1.32	F5V	0.04	1.25	0.01	0.05	0.08
18	WASP-3 b	1.76	1.31	0.97	1.24	F7V	0.03	1.6	0.31	1.79	2.93
19	WASP-7 b	0.96	0.92	1.56	1.28	F5V	0.06	1.21	0.07	0.4	0.67
20	X0-3 b	11.79	1.22	8.12	1.21	F5V	0.05	1.15	0.002	0.01	0.019
21	X0-4 b	1.72	1.34	0.89	1.32	F5V	0.06	1.3	0.09	0.52	0.87
G											
22	CoRoT-Exo-1 b	1.03	1.49	0.37	0.95	G0V	0.03	2.36	1.3	6.99	10.81
23	CoRoT-Exo-2 b	3.31	1.47	1.31	0.97	G	0.03	1.56	0.06	0.35	0.59
24	HAT-P-1 b	0.52	1.23	0.35	1.13	G0V	0.06	1.43	0.32	1.88	3.07
25	HD 149026 b	0.36	0.65	1.59	1.3	G0IV	0.04	1.32	0.16	0.93	1.53
26	HD 17156 b	3.21	1.02	3.72	1.24	G0	0.16	1.05	0.0004	0.003	0.004
27	HD 209458 b	0.69	1.32	0.37	1.01	G0V	0.05	1.49	0.34	1.98	3.23
28	OGLE-TR-10 b	0.63	1.26	0.39	1.18	G	0.04	1.61	0.48	2.76	4.46
29	OGLE-TR-56 b	1.29	1.3	0.73	1.17	G	0.02	2.2	0.6	3.45	5.53
30	SWEEPS-11	9.7	1.13	8.34	1.1	G ^x	0.03	1.24	0.002	0.01	0.02
31	TrES-2	1.2	1.22	0.82	0.98	G0V	0.04	1.47	0.14	0.83	1.36
32	TrES-3	1.92	1.3	1.1	0.92	G	0.02	1.81	0.22	1.26	2.08
33	WASP-4 b	1.12	1.42	0.49	0.9	G7V	0.02	2.32	1.09	5.97	9.33
34	WASP-5 b	1.58	1.09	1.51	0.97	G4V	0.03	1.55	0.11	0.68	1.12
35	WASP-6 b	0.5	1.22	0.34	0.88	G8	0.04	1.57	0.66	3.76	6.04
36	X0-1 b	0.9	1.18	0.67	1	G1V	0.05	1.35	0.12	0.69	1.15
37	X0-5 b	1.08	1.09	1.04	0.88	G8V	0.05	1.28	0.06	0.36	0.59
K											
38	HAT-P-11 b	0.08	0.42	1.34	0.81	K4	0.05	1.22	0.16	0.97	1.59
39	HAT-P-3 b	0.6	0.89	1.05	0.94	K	0.04	1.38	0.07	0.41	0.68
40	HD 189733 b	1.13	1.14	0.95	0.8	K1-K2	0.03	1.51	0.07	0.42	0.70
41	Lupus-TR-3 b	0.81	0.89	1.43	0.87	K1V	0.05	1.26	0.02	0.15	0.24
42	OGLE-TR-111 b	0.53	1.07	0.54	0.82	K	0.05	1.37	0.10	0.62	1.02
43	OGLE-TR-113 b	1.32	1.09	1.27	0.78	K	0.02	1.69	0.1	0.56	0.93
44	TrES-1	0.61	1.08	0.6	0.87	K0V	0.04	1.48	0.13	0.76	1.26
45	WASP-10 b	3.06	1.08	3.01	0.71	K5	0.04	1.23	0.01	0.03	0.05
46	WASP-11 b	0.46	1.05	0.5	0.82	K3V	0.04	1.43	0.15	0.91	1.51
47	WASP-2 b	0.88	1.02	1.04	0.84	K1V	0.03	1.5	0.08	0.49	0.82
48	X0-2 b	0.57	0.97	0.77	0.98	K0V	0.04	1.48	0.12	0.71	1.18
M											
49	GJ 436 b	0.07	0.44	1.06	0.45	M2.5	0.03	1.41	0.43	2.51	4.08

because the X-ray flux from cooler stars is significantly lower than the flux from solar-mass stars for a given orbital distance.

One can see from Table 1 that the Roche Lobe has an important influence on the atmospheric mass loss of close-in exoplanets. Fig. 4 shows the Roche lobe related mass enhancement

factor ζ as a function of planetary density ρ and orbital distance around early M-type stars with $M_{\text{Star}} = 0.5M_{\text{Sun}}$ and Sun type stars with $M_{\text{Star}} = 1.0M_{\text{Sun}}$. One can see from Fig. 4 that close-in exoplanets with low densities are more affected compared to similar planets with a higher density. Our study indicates also

that the Roche lobe effect is more efficient around G-type stars compared to lower mass stars. One can see from Fig. 4 that the

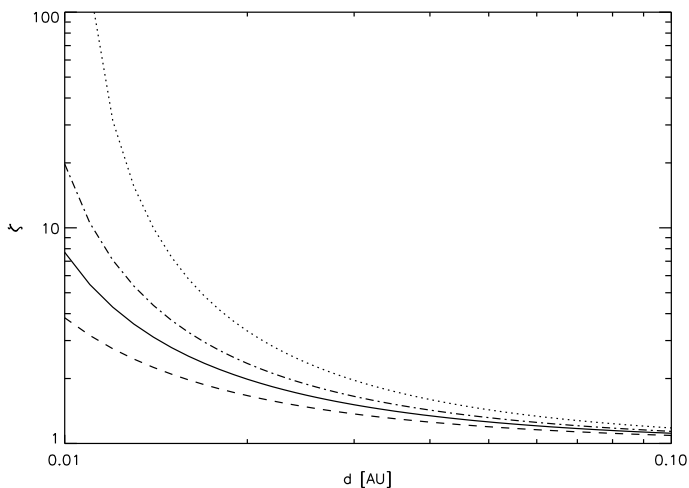


Fig. 4. Roche lobe related mass enhancement factor ζ as a function of orbital distance for exoplanets with a density of 0.4 g cm^{-3} (dot-dashed line) and 1.3 g cm^{-3} (dashed line) around a M star with a mass of $0.5 M_{\text{Sun}}$. The dotted line and solid line correspond for similar dense planets around a G star with one solar mass.

Roche lobe effect enhances the mass loss at orbital distances $\leq 0.02 \text{ AU}$ dramatically. Exoplanets with densities which are $\leq 0.55 \text{ g cm}^{-3}$ can lose their initial hydrogen inventory if they orbit around G-type stars at distances of about 0.01 AU . Baraffe et al. (2004) compared the ratio of the mass loss timescale t_{M} to the thermal timescale t_{th} , which is characterized by the Kelvin-Helmholtz timescale and found that, when $t_{\text{M}}/t_{\text{th}}$ becomes < 1 the evolution of “Hot Jupiters” changes drastically which results in rapid expansion of the planetary radius and enhances the mass loss. Our model results indicate that close-in hydrogen-rich gas giants at orbital distances $\leq 0.015 \text{ AU}$ may experience this violent mass loss effect.

Table 2 shows the integrated mass loss over 4 Gyr for gas giants with 1.0 and $0.5 M_{\text{Jup}}$ and a “Hot Neptune” and densities of 0.4 and 1.241 g cm^{-3} in orbital distances between 0.01 – 0.025 AU around G stars.

One can see from Table 2 that thermal evaporation may be an efficient loss process which can efficiently evaporate the dense hydrogen envelopes of close-in exoplanets in the Neptune-mass domain at orbital distances $d < 0.025 \text{ AU}$ around G-type stars. Jupiter-mass exoplanets with high densities ($> 1 \text{ g cm}^{-3}$) experience negligible thermal atmospheric mass loss at orbital distances beyond $\geq 0.015 \text{ AU}$. Between 0.01 – 0.015 AU similar gas giants may lose $\leq 10 \%$ of their initial atmosphere. In agreement with Fig. 4, low density gas giants can significantly lose their hydrogen atmospheres at 0.01 AU . Gas giants with masses of $\sim 0.5 M_{\text{Jup}}$ and densities of about 1.25 g cm^{-3} can lose about 16% of their mass at G-star orbital distances of about 0.01 AU . We note also that the majority of the thermal mass loss occurs during the first Gyr when the XUV radiation of the young stars is much higher compared to ages beyond 1 Gyr after the stars origin. The same exoplanets would experience lower mass loss if the orbits are located at similar distances around K-type stars.

One can also see from Table 2 that the recently discovered transiting “Super-Earth” CoRoT-Exo-7 b, which is located around an orbit of a K star at about 0.017 AU can not be the remaining core of an evaporated “Hot Jupiter”. For instance a low

density ($\rho_{\text{pl}} \sim 0.4 \text{ g cm}^{-3}$) gas giant around a K star at an orbital distance of about 0.017 AU and a mass of about $0.5 M_{\text{Jup}}$ loses with a heating efficiency of 60% after 4 Gyr $\sim 23 \%$ of its initial mass. If one considers the energy-limited loss ($\eta = 100\%$) the same planet would lose about 46% of its mass. On the other hand a “Hot Neptune” with a low density at the same orbital distance could lose its hydrogen envelope so that the planet’s core remain. We can therefore not rule out that CoRoT-Exo-7 b is not a remnant of an evaporated “Hot Neptune” or sub-Neptune-class object.

Fig. 5 shows the effect of thermal mass loss for two gas giants with an initial mass of $0.5 M_{\text{Jup}}$ and densities of $\rho_1 = 1.24 \text{ g cm}^{-3}$ and $\rho_2 = 0.4 \text{ g cm}^{-3}$ at 0.02 AU (EGP I) and 0.025 AU (EGP II) in an area where so far no Jupiter-mass or sub-Jupiter-class exoplanets were discovered. The circles represent the mass evolution of the test planets after 4 Gyr for both densities ρ_1 and ρ_2 . The dashed line separates discovered exoplanets in the mass range between 0.01 – $1.0 M_{\text{Jup}}$ from the area where no exoplanets have been discovered so far. As one can see thermal atmospheric mass loss is not efficient enough to evaporate gas giants which should be located in this area down to their core sizes. If this gap of exoplanets is related to mass loss non-thermal processes have to be responsible.

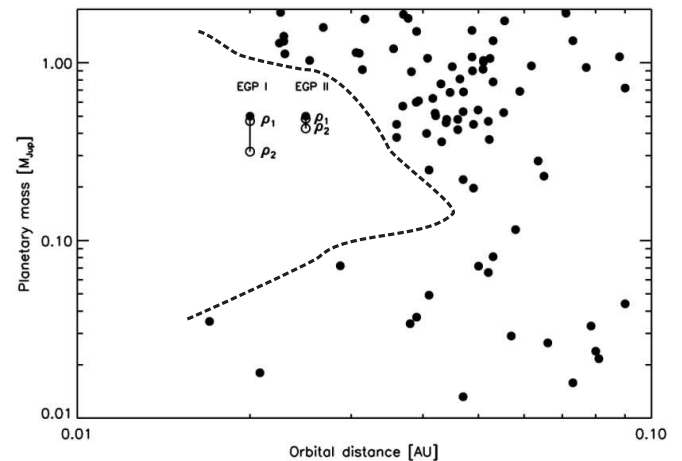


Fig. 5. Illustration of thermal mass loss integrated over 4 Gyr for low ($\rho_2 = 0.4 \text{ g cm}^{-3}$) and high ($\rho_1 = 1.24 \text{ g cm}^{-3}$) density gas giants with initial masses of $0.5 M_{\text{Jup}}$ located in an area where no exoplanets have been discovered until now. The filled circles show discovered exoplanets in mass range between 0.01 – $1.0 M_{\text{Jup}}$ and an orbital distance between 0.01 – 0.1 AU .

In the following section we investigate if stellar wind and CME plasma induced non-thermal atmospheric erosion can effectively modify the mass evolution of non- or weakly magnetized gas giants in orbital distances $\leq 0.1 \text{ AU}$.

3. Atmospheric mass loss related to stellar wind and CME induced ion erosion

Taking into account that tidal-locking of short periodic exoplanets may result in weaker intrinsic magnetic moments, as compared to fast rotating Jupiter-class exoplanets at larger orbital distances (Grießmeier et al. 2004), and Khodachenko et al. (2007) found that the encountering of dense stellar wind and CME plasma may compress the magnetosphere and force the

Table 2. The mass loss of “Hot Jupiters” and “Hot Neptunes” with low and high densities at four different orbital distances around a G star ($1M_{\text{Sun}}$) and a K star ($0.8M_{\text{Sun}}$).

$M_{\text{pl}}/M_{\text{Jup}}$		$\rho_{\text{pl}}/\rho_{\text{Jup}}$	$\Delta M_{\text{pl}}/M_{\text{pl}}^{10\%}$	$\Delta M_{\text{pl}}/M_{\text{pl}}^{60\%}$	$\Delta M_{\text{pl}}/M_{\text{pl}}^{100\%}$	$\Delta M_{\text{pl}}/M_{\text{pl}}^{10\%}$	$\Delta M_{\text{pl}}/M_{\text{pl}}^{60\%}$	$\Delta M_{\text{pl}}/M_{\text{pl}}^{100\%}$
0.01 AU			mass loss [%] (G stars)			mass loss [%] (K stars)		
1	1.24		7.40	-	-	2.3	14.97	27.72
0.5	1.24		15.83	-	-	4.66	36.12	-
0.054	1.61		-	-	-	38.36	-	-
1	0.4		-	-	-	-	-	-
0.5	0.4		-	-	-	-	-	-
0.054	0.4		-	-	-	-	-	-
0.017 AU								
1	1.24		0.8	4.88	8.27	0.31	1.85	3.09
0.5	1.24		1.6	10.0	17.38	0.61	3.72	6.28
0.054	1.61		12.06	-	-	4.46	31.16	72.73
1	0.4		4.79	37.0	-	1.65	10.41	18.23
0.5	0.4		9.9	-	-	3.34	22.55	45.68
0.054	0.4		-	-	-	51.26	-	-
0.020 AU								
1	1.24		0.49	2.97	5.0	0.19	1.15	1.93
0.5	1.24		0.98	6.03	10.25	0.38	2.32	3.89
0.054	1.61		7.35	66.69	-	2.82	18.24	33.21
1	0.4		2.43	15.77	28.76	0.89	5.47	9.30
0.5	0.4		4.93	36.78	-	1.79	11.29	19.76
0.054	0.4		-	-	-	20.44	-	-
0.025 AU								
1	1.24		0.27	1.61	2.69	0.11	0.64	1.06
0.5	1.24		0.53	3.23	5.44	0.21	1.28	2.13
0.054	1.61		4.0	27.09	54.26	1.57	9.79	16.89
1	0.4		1.13	7.0	11.98	0.44	2.63	4.43
0.5	0.4		2.28	14.58	26.03	0.87	5.33	9.04
0.054	0.4		26.99	-	-	9.19	-	-

magnetospheric standoff location down to heights where ionization and ion pick-up of the planetary neutral atmosphere by the CME plasma flow takes place. Here a planetary ionosphere represents the thermal plasma which is produced by the interaction of the stellar XUV radiation with the neutral atmosphere and which is controlled by the gravity and magnetic field of the planet.

Back to our Solar System, it is known that magnetosphere-like structures are found at all planets regardless if the planet has an intrinsic global magnetic field or not. The solar wind interaction with a planet produces a magnetosphere-like structure near the planet with common features such as bow shock, magnetosheath, magnetotail, and boundary layers. In the case of intrinsically magnetized planets like the Earth, a magnetosphere is formed to stand-off the oncoming solar wind.

For a planet like Venus or Mars, which has no global intrinsic magnetic field but an atmosphere, an induced magnetosphere is created by the magnetized solar wind interaction with the highly conducting ionosphere. The induced magnetosphere is therefore analogous to the magnetosphere of an intrinsically magnetized planet, but occupies a smaller volume (Zhang et al. 2007). We note that in the case of Mars or Venus, the ionospheric pressure is mostly larger or comparable with the solar wind ram pressure, both in solar wind maximum and minimum. The interaction of the post-shock solar wind flow with the ionosphere results in a distinct boundary. This is the so-called ionopause which confines the thermal plasma of the ionosphere and marks its top boundary (cf., Phillips and McComas 1991).

Whether the stellar wind is stopped well above the planet depends on the pressure balance between the stellar wind ram pressure ($p_{\text{sw}} = \rho_{\text{sw,CME}} v_{\text{sw,CME}}^2$) and the maximum ionospheric thermal pressure ($p_{\text{ion}} = n_{\text{ik}}(T_{\text{e}} + T_{\text{i}})$). To the first order, here we simply compare the stellar wind ram pressure with the peak ionospheric pressure to determine the height where the stellar wind would be stood off. It is reasonable to postulate that the stellar wind will be absorbed by the planetary atmosphere if the ram pressure is larger than the ionospheric pressure. Such an extreme plasma-atmosphere interaction could result in a large atmospheric mass loss due to ion pick up and other non-thermal escape processes.

Thus, by using this analogy we can expect that the ionosphere of non- or weakly magnetized “Hot Jupiters” represents an obstacle similar to that where a magnetosphere is present. The difference between the ionized and the magnetic obstacle may be their distance above the visual radius of the planet.

Fig. 6 illustrates the stellar plasma interaction with non- or weakly magnetized gas giants. The dashed-line corresponds to the critical ionopause location (IP_{c}) at about $1.5r_{\text{pl}}$ above the visual radii. The H^+ ion pick up loss rate for a Jupiter-type gas giant at 0.045 AU at about $1.5r_{\text{pl}}$ above the visual radii is in the order of about 10^{13} g s^{-1} (Khodachenko et al. 2007) and lower at higher IP locations where pick up ion losses become comparable with the thermal loss rate of “Hot Jupiters” but negligible if one integrates this value over the life time of the planet. If the stellar plasma flow interacts below this critical boundary, the mass loss rate of a “Hot Jupiter” ($M_{\text{pl}} \ll M_{\text{Jup}}$) becomes larger and can

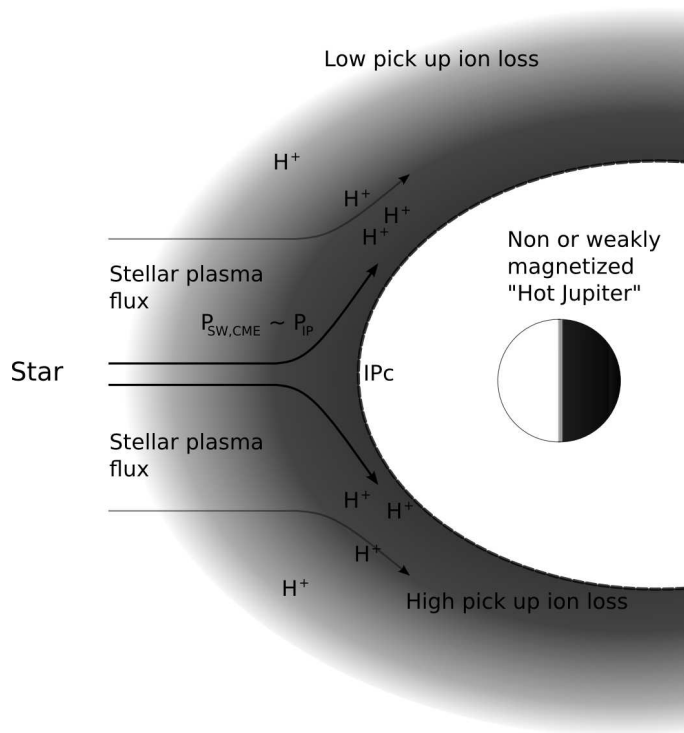


Fig. 6. Illustration of the stellar plasma interaction with non- or weakly magnetized gas giants.

probably erode the planet’s hydrogen inventory (Khodachenko et al. 2007).

Thus, from the study of Khodachenko et al. (2007) we know that ion pick up loss is negligible for “Hot Jupiters” if a planetary obstacle builds up at atmospheric distances $\geq 1.5r_{pl}$ (shaded area in Fig. 6). For studying the stellar wind and CME ram pressure as well as the ionospheric pressure of “Hot Jupiters” one has to know the stellar wind and CME plasma density and velocity as a function of orbital distance, as well as the ionospheric density profile, and the ion temperature and electron temperature of “Hot Jupiters”.

By considering that the Sun is a typical G-type star, we assume a similarity of the basic parameters and their spatial behavior for the stellar wind on other G-type stars and those in the solar wind. In view of the limited amount of precise quantitative information regarding the stellar (non-solar) winds such a solar-stellar analogy principle is widely used for the investigation of basic processes of the stellar wind - planetary interactions. Therefore, in the present study we use the Sun as a proxy for estimating the stellar wind and CME density and speed dependence as a function of the orbital distance d . In particular, for the approximation of the stellar wind density we use the empirical power-law formula

$$n_{sw} = \left(1.07 \frac{d}{R_{Sun}}^{-3.1} + 19.94 \frac{d}{R_{Sun}}^{-6.06} + 22.10 \frac{d}{R_{Sun}}^{-12.93} \right) \times 10^7, \quad (11)$$

which was derived from Skylab coronagraph observations (Guhathakurta et al. 1996). The stellar wind and CMEs speed can be approximated by

$$v_{sw}^2 = v_0^2 \cdot (1 - e^{(2.8-d)/8.1}), \quad (12)$$

developed by Sheeley et al. (1997) on the basis of tracking several solar wind density enhancements at close distances ($d < 0.1$

AU). For the stellar wind speed one can take in this formula $v_0 = 300 \text{ km/s}$, whereas for average and fast CMEs one can use $v_0 = 500 \text{ km/s}$ and 800 km/s . The decrease of the average CME plasma density n_{CME} at orbital distances $d \leq 0.1 \text{ AU}$ is described by $n_{CME}(d) = n_0(d/d_0)^{-3.6}$, which for $n_0 = 2 \times 10^6 \text{ cm}^{-3}$ and $d_0 = 3R_{Sun}$ gives a good approximation for the values estimated from the SOHO/LASCO coronagraph images (Lara et al. 2004). These power-law approximations of the CME density follow from the analysis of solar CME-associated brightness enhancements in the white-light coronagraph images (e.g., Khodachenko 2007, and references therein). The average mass of CMEs, is $\approx 10^{15} \text{ g}$ and the average duration of CMEs, at distances $(6 \dots 10)R_{Sun}$ is $\approx 8 \text{ h}$.

Fig. 7 shows the resulting stellar wind and CME plasma parameters as well as the corresponding ram pressures. Table 3 summarizes particular values of the stellar wind and CME plasma parameters obtained from these approximations for the given orbital distances 0.015 AU, 0.045 AU and 0.1 AU. For estimating the ionopause pressure of assumed non- or weakly magnetized “Hot Jupiters” we use the H^+ ion profiles and temperatures modeled by Yelle (2004). This author applied a coupled photochemical and hydrodynamic model on hydrogen-rich atmospheres of “Hot Jupiters” in orbits with semi-major axes from 0.01 to 0.1 AU. The modeled planetary plasma parameters correspond to planetary distances of about $3r_{pl}$ and are shown in Table 4.

One can see that the ionosphere density increases if the hydrogen-rich gas giant is located at closer orbital distance. This ion enrichment is related to higher stellar XUV flux closer to the star. Exoplanets at closer orbital distance are exposed to more extreme stellar plasma flows but on the other hand the upper atmospheres of planets under such extreme conditions are also much stronger ionized. By using the stellar and planetary plasma parameters shown in Table 3 we estimate the corresponding ram and planetary ion pressures which are summarized in Table 4.

As one can see from Table 4, the ion pressure of “Hot Jupiters” can easily balance the incoming stellar wind and average expected CME ram pressures at $\sim 2r_{pl}$, that is close but above the critical ion pick up erosion distance of about $1.5r_{pl}$. We note that a factor of 2 related to the ionopause pressure is within the uncertainties of atmospheric/ionospheric model assumptions. From this estimation we can conclude that the ionopause of “Hot Jupiters” when they are exposed to ordinary stellar winds or average CMEs will form at locations, where such a massive exoplanet is not strongly eroded by the stellar plasma flow. On the other hand one can also see from Table 4 that the ion pressure is not able to balance the ram pressure of fast CMEs between orbital distances of $\sim 0.02\text{--}0.1 \text{ AU}$.

One can see from panel (b) in Fig. 7, the CMEs reach their highest speed at about 0.02 AU, therefore the ram pressure is lower at orbital distances which are $\leq 0.02 \text{ AU}$. Interestingly the orbital distance where fast CMEs should efficiently erode the atmospheres of “Hot Jupiters” corresponds to the orbital distance shown in Fig. 5 where so far no exoplanets within the mass range between $0.1M_{Jup}\text{--}1.0M_{Jup}$ are discovered. One may wonder if this is a coincidence or if fast CMEs are responsible for the missing “Hot Jupiters” between 0.02–0.035 AU (see Fig. 5). In future studies we plan to investigate if fast CMEs could be a reason for the missing exoplanet population within the above mentioned mass range and orbital distances.

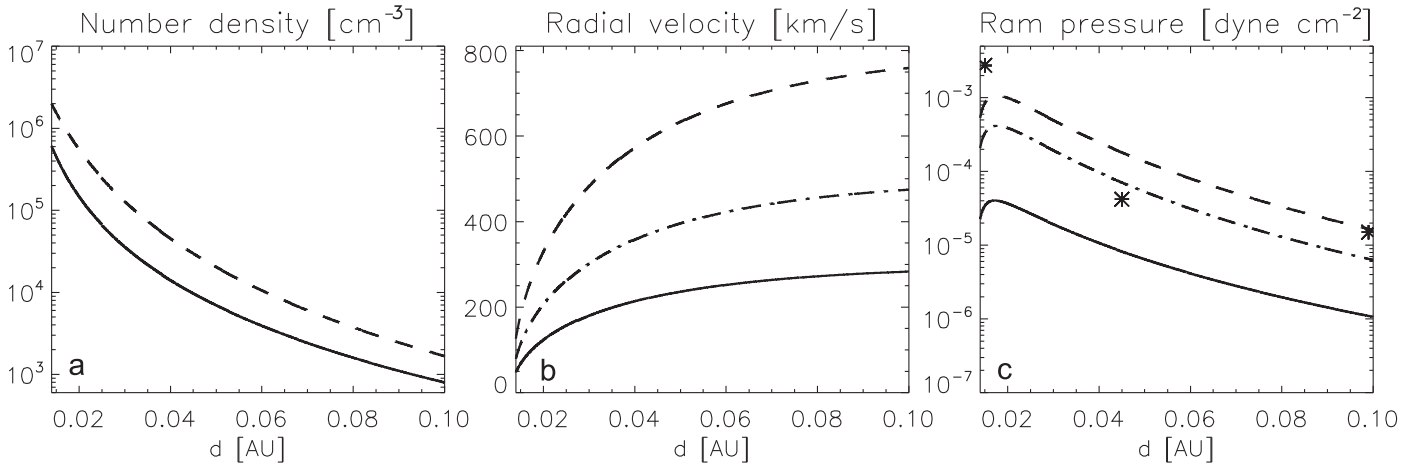


Fig. 7. Stellar wind and CME parameters versus orbital distance corresponding to a Sun-like G star. a) Density: stellar wind (solid line), CME (dashed line); b) Radial velocity: stellar wind (solid line), fast CME (dashed line), average CME (dashed-dotted line); c) Ram pressure: stellar wind (solid line), fast CME (dashed line), average CME (dashed-dotted line).

d [AU]	n_{sw} [cm ⁻³]	v_{sw} [km/s]	n_{CME} [cm ⁻³]	v_{CME}^{av} [km/s]	v_{CME}^{fast} [km/s]	n_{H^+} [cm ⁻³]	$T_i + T_e$ [K]
0.1	794	283	1667	474	759	6×10^6	2.0×10^4
0.045	9625	226	2.95×10^4	378	605	1×10^7	3.0×10^4
0.015	4.48×10^5	68	1.54×10^6	113	181	4×10^8	5.0×10^4

Table 3. Stellar wind and planetary plasma parameters.

d [AU]	P_{sw} [10^{-7} dyne cm ⁻²]	P_{CME}^{av} [10^{-7} dyne cm ⁻²]	P_{CME}^{fast} [10^{-7} dyne cm ⁻²]	P_{ion} [10^{-7} dyne cm ⁻²]
0.1	11.0	63.0	160.0	150.0
0.045	82.0	705.0	1805.0	420.0
0.015	341.0	3294.0	8432.0	5500.0

Table 4. Dynamic stellar plasmas and planetary ion pressures.

4. Conclusion

We applied a modified energy-limited mass loss equation which can reproduce the full hydrodynamic approach of Penz et al. (2008) for the study of the thermal mass loss of 49 known transiting exoplanets over 4 Gyr. We note also that previous thermal atmospheric mass loss evolution studies like that of Lammer et al. (2003), Baraffe et al. (2004) and Lecavelier Des Etangs (2007), which applied energy-limited formulas but neglected that the heating efficiency is substantially less than 100 % overestimated the mass loss rates. We studied the initial mass of these exoplanets and found that for the given planetary and stellar parameters only the low density “Hot Jupiter” WASP-12 b could have lost about 24 % of its initial mass. There are also several transiting planets like the low density exoplanet CoRoT-1 b which lost about 5–7 % of their initial masses. The thermal mass loss of close-in gas giants can be very efficient at orbital distances ≤ 0.02 AU. Most of the observed transiting exoplanets experienced negligible mass loss during their life time. Compared with high density exoplanets, low density gas giants are affected much stronger against thermal mass loss. The mass loss enhancing effect of the Roche lobe together with low planetary densities are the main factors for high mass loss rates. Depending on the heating efficiency, low density Neptune-class objects can lose their hydrogen envelopes at orbital distances ≤ 0.045 AU.

Our study indicates that one can rule out that the first discovered transiting “Super-Earth” CoRoT-Exo-7 b is a remnant of a

thermally evaporated hot gas giant. But one can not rule out that CoRoT-Exo-7 b is the core of a low density Neptune-class or sub-Neptune-class exoplanet which lost its hydrogen envelope. Owing to the XUV flux evolution and Roche lobe effect, the thermal mass loss is lower on exoplanets orbiting low mass stars, compared to planets in similar orbital distances around G or F type stars. We found that non-thermal stellar plasma induced H^+ pick up erosion on a non- or weakly magnetized “Hot Jupiter” is most likely negligible if such a planet interacts with the ordinary stellar wind or average CMEs. Due to the large stellar XUV flux, extended ionospheres are produced. The ion pressure of these ionospheres is strong enough that the stellar wind and CME ram pressure can be balanced at distances of a few planetary radii, resulting in negligible atmospheric erosion rates over evolutionary time scales. Fast CMEs however, can not be balanced by the planetary ion pressure at orbital distances between ~ 0.02 – 0.1 AU. During such collisions “Hot Jupiters” may experience high non-thermal escape rates. Future research on fast CME interaction with “Hot Jupiters” will help us to understand if such extreme events are behind the phenomenon that no gas giants with masses $< 1.0M_{Jup}$ are discovered so far at orbital distances ≤ 0.035 AU. Finally we conclude that the results of our study show that the discovery of transiting exoplanets at orbital distances ≤ 0.015 AU and ground-based follow-up mass determinations together with theoretical mass loss studies can bring reliable information on the statistics of remaining cores of shrunk gas giants.

Acknowledgements. H. Lammer, P. Odert, M. Leitzinger, M. L. Khodachenko and A. Hanslmeier gratefully acknowledge the Austrian Fonds zur Förderung der wissenschaftlichen Forschung (FWF grant P19446) for supporting this project. M. Panchenko and M. L. Khodachenko acknowledge also the Austrian Fonds zur Förderung der wissenschaftlichen Forschung (project P20680-N16). H. Lammer, H. I. M. Lichtenegger, Yu. N. Kulikov and N. V. Erkaev thank the AAS “Verwaltungsstelle für Auslandsbeziehungen” and the RAS. H. Lammer, H. I. M. Lichtenegger, M. L. Khodachenko and Yu. N. Kulikov acknowledge support from the Helmholtz-Gemeinschaft as this research has been supported by the Helmholtz Association through the research alliance “Planetary Evolution and Life”. H. Lammer, M. L. Khodachenko, T. Penz, and Yu. N. Kulikov also acknowledge the International Space Science Institute (ISSI; Bern, Switzerland) and the ISSI teams “Evolution of Habitable Planets” and “Evolution of Exoplanet Atmospheres and their Characterization”. The authors also acknowledge fruitful discussions during various meetings related to the Europlanet N2 activities as well as within the N2 Exoplanet discipline working group DWG 7. T. Penz and G. Micela acknowledges support by the Marie Curie Fellowship Contract No. MTKD-CT-2004-002769 of the project “The influence of stellar high radiation on planetary atmospheres”. The authors also thank the Austrian Ministry bm:bwk and ASA for funding the CoRoT project.

References

- Baraffe, I., Selsis, F., Chabrier, G., et al. 2004, *A&A*, 419, L13
 Burrows, A., Guillot, T., Hubbard, W. B., et al. 2000, *ApJ*, 534, L97
 Chassefiere, E. 1996, *J. Geophys. Res.*, 101, 26039
 García Muñoz, A. 2007, *Planet. Space Sci.*, 55, 1426
 Erkaev, N. V., Penz, T., Lammer, H., et al. 2005, *ApJS*, 157, 396
 Erkaev, N. V., Kulikov, Yu., Lammer, H., et al. 2007, *A&A*, 472, 329
 Evans, J. V. 1977, *Rev Geophys*, 15, 325
 Grießmeier, J.-M., Stadelmann, A., Penz, T., et al. 2004, *A&A*, 425, 753
 Guhathakurta, M., Holzer, T. E., & MacQueen, R. M. 1996, *ApJ*, 458, 817
 Guillot, T. 2005, *Ann. Rev. Earth Planet. Sci.*, 33, 493
 Khodachenko, M. L., Lammer, H., Lichtenegger, H. I. M. et al. 2007, *Planet Space Sci.*, 55, 631
 Kliore, A. J. & Luhmann, J. G. 1997, *J Geophys Res*, 96, 21,281
 Lammer, H., Selsis, F., Ribas, I., et al. 2003, *ApJ*, L121, 598
 Lammer, H., Lichtenegger, H. I. M., Biernat, H. K. et al. 2006, *Planet. Space Sci.*, 54, 1445
 Lara, A., González-Esparza, J. A., & Gopalswamy, N. 2004, *Geofísica Internacional*, 43, 75
 Lecavelier des Etangs, A., Vidal-Madjar, A., McConnell, J. C., & Hébrard, G. 2004, *A&A*, 418, L1
 Lecavelier des Etangs, A. 2007 *A&A*, 461, 1185
 Penz, T., Erkaev, N. V., Kulikov, Yu. N., et al. 2008a, *Planet. Space Sci.*, 56, 1260
 Penz, T., Micela, G., Lammer, H. 2008b, *A&A*, 477, 309
 Penz, T., & Micela, G. 2008, *A&A*, 479, 579
 Phillips, J. L., & McComas, D. J. 1991, *Space Sci. Rev.*, 55, 1
 Preibisch, T. & Feigelson, E. D., 2005, *ApJS*, 160, 390
 Ribas, I., Guinan, E. F., Güdel, M., & Audard, M. 2005, *ApJ*, 622, 680
 Sheeley, N. R., Jr., Wang, Y.-M., Hawley, S. H., Brueckner, G. E., Dere, K. P., Howard, R. A., Koomen, M. J., Korendyke, C. M., Michels, D. J., Paswaters, S. E., Socker, D. G., St. Cyr, O. C., Wang, D., Lamy, P. L., Llebaria, A., Schwenn, R., Simnett, G. M., Plunkett, S., Biesecker, D. A. 1997, *ApJ*, 484, 472
 Sekiya, M., Nakazawa, K., Hayashi, C. 1980, *Earth Planet. Sci. Lett.*, 50, 197
 Sekiya, M., Nakazawa, K., Hayashi, C. 1980, *Prog. Theoret. Phys.*, 64, 1968
 Sekiya, M., Hayashi, C., Nakazawa, K. 1981 *Prog. Theoret. Phys.*, 66, 1301
 Tian, F., Toon, O. B., Pavlov, A. A., & Sterck, H. De. 2005, *ApJ*, 621, 1049
 Vidal-Madjar, A., Lecavelier Des Etangs, A., Desert, J.-M., Ballester, G. E., Ferlet, R., Hébrard G. & Mayor, M. 2003, *Nature*, 422, 143
 Watson, A. J., Donahue, T. M., Walker, J. C. G. 1981, *Icarus*, 48, 150
 Wuchterl, G., Broeg, C., Krause, S., & Pecnik, B. 2007, *arXiv:astro-ph/0701003*
 Yamauchi M., & Wahlund J.-E. 2007, *Astrobiology*, 7, 783
 Yelle, R. V., 2004, *Icarus*, 170, 167
 Yelle, R. V., 2006, *Icarus*, 183, 508
 Zhang, M. H. G., Luhmann, J. G., Kliore, A. J., & Russell, C. T. 1990, *J. Geophys Res* 95, 14,829
 Zhang, T. L., Delva, M., Baumjohann, W. et al. 2007, *Nature*, 450, 654